Title

Feasibility study of high spatial resolution multimodality fluorescence tomography in ex vivo biological tissue.

Journal

Applied Optics, 56(28)

ISSN

1559-128X

Authors

Kwong, Tiffany C

Nouizi, Farouk

Cho, Jaedu

et al.

Publication Date

2017-10-01

DOI

10.1364/ao.56.007886

Peer reviewed

Published in final edited form as:

Appl Opt. 2017 October 01; 56(28): 7886–7891. doi:10.1364/AO.56.007886.

Feasibility study of high spatial resolution multimodality fluorescence tomography in *ex vivo* biological tissue

TIFFANY C. KWONG[1,*], **FAROUK NOUIZI**[1], **JAEDU CHO**[1], **YUTING LIN**[1,2], **UMA SAMPATHKUMARAN**[3], **GULTEKIN GULSEN**[1]

[1]Tu and Yuen Center for Functional Onco-Imaging, Department of Radiological Sciences, University of California, Irvine, California 92697, USA

[2]Department of Radiation Oncology, Duke University, Durham, North Carolina 27708, USA

[3]InnoSense LLC, Torrance, California 90505, USA

Abstract

Previously, we demonstrated that temperature-modulated fluorescence tomography (TM-FT) could provide fluorescence images with high quantitative accuracy and the spatial resolution of focused ultrasound. TM-FT is based on scanning the focused ultrasound across the medium to activate temperature-reversible fluorescent nanoprobes (ThermoDots). This technique can resolve small fluorescent targets located several centimeters deep in turbid media with millimeter resolution. Our past studies with this multimodality technique used agar phantoms, which could not represent the true heterogeneous nature of the acoustic and optical properties of biological tissue. In this work, we report the results of the first TM-FT study performed on *ex vivo* chicken breast tissue. In order to improve the spatial resolution of this technique, diffuse optical tomography is also used to better estimate the optical property maps of the tissue, which is utilized as functional a priori for the TM-FT reconstruction algorithm. These *ex vivo* results show that TM-FT can accurately recover the concentration and position of a 1.5 mm × 5 mm inclusion filled with ThermoDots. Since the inclusion is embedded 2 cm deep in the chicken breast sample, these results demonstrate the great potential of TM-FT for future *in vivo* small animal imaging.

Keywords

(110.7050) Turbid media; (260.2510) Fluorescence; (110.6955) Tomographic imaging; (170.0110) Imaging systems; (170.3880) Medical and biological imaging; (170.0170) Medical optics and biotechnology

1. INTRODUCTION

Fluorescence diffuse optical tomography (FDOT or FT) is a safe, inexpensive imaging technique that uses near-infrared (NIR) light to image biological tissue. FT can noninvasively provide the concentration and position of a fluorophore located several centimeters deep in the tissue. Although this technique has become increasingly popular in

*Corresponding author: tckwong@uci.edu.

preclinical imaging to provide molecular information, its applications are severely limited by the ill-posed and undetermined nature of the FT inverse problem [1]. Indeed, strong scattering in biological tissue makes it impossible to focus direct light beyond one mean transport free path (~1 mm) [2]. As a result, achieving high spatial resolution and quantitatively accurate fluorescence images in tissue, more than a few millimeters deep, is unattainable with diffuse optical techniques alone. Consequently, the addition of spatial a priori information obtained from a structural imaging modality, such as magnetic resonance imaging (MRI) or x-ray computed tomography (CT), has been shown to considerably improve the spatial resolution and accuracy of the FT image reconstruction by providing the position of the fluorescent target [3,4]. However, this method fails if the position found by the structural imaging modality does not exactly match the true fluorescent distribution [5]. As cancer progresses, for example, a tumor can outgrow its original blood supply, leading to cell death and necrosis in the interior of the tumor. Hence, using the tumor boundary derived from x-ray CT or MRI will result in error, as these anatomical imaging modalities lack the sensitivity to provide functional information about the location of the viable tissue and where the fluorophore is delivered.

In addition, while combing FT with other techniques can improve the spatial resolution, FT ultimately depends on the specificity of the fluorescent probe that is designed to respond to a specific stimulus or to location within a specific region of a biological specimen. Although indocyanine green (ICG) is currently the only NIR fluorophore FDA approved for medical diagnosis and can accumulate in cancer tumors due to the vascular permeability of cancer blood vessels, its applications are limited due to its thermal, photo, and aqueous instability [6]. Not only is ICG amphiphilic and degrades in aqueous solution, but it also has a tendency to aggregate and quench in solution, leading to a lower fluorescence quantum yield [6]. Consequently, there has been much interest in the development of targeted or activatable probes to counteract the limited delivery, accumulation, and retention of ICG alone.

Recently, temperature-sensitive fluorescence contrast agents have been reported using ICG-loaded pluronic micelles [7–9]. Pluronic polymers such as Pluronic-F127 exhibit a unique thermo-reversible behavior allowing it to self-assemble into a micelle in aqueous solution. As the temperature changes, the interiors of micelles change their hydrophobicity/hydrophilicity, which in turn yields a change in the micelle size and ICG concentration and is responsible for the changes in the fluorescence quantum yield [7–9]. The temperature dependence of these contrast agents provides a major opportunity to overcome the spatial resolution limitation of conventional fluorescence imaging by using temperature modulation.

Previously, we introduced a new method to avoid the use of mismatched anatomical/fluorescent information, termed “temperature modulated fluorescence tomography (TM-FT)” [10]. This technique utilizes focused ultrasound to provide localized heating, and our unique activatable thermo-reversible fluorescent nanoprobes (ThermoDots) whose quantum efficiency and lifetime increase with temperature [11]. TM-FT can provide fluorescent images beyond the diffusion limit, by providing a binary map of the position of the ThermoDots with focused ultrasound resolution (~1.33 mm) [11]. In this technique, the focused ultrasound is scanned across the medium while optical measurements are acquired. The resulting increase in the ThermoDots’ fluorescence signal following activation by the

focused ultrasound is then used to localize their position and produce a binary map of the fluorophore distribution. Thus, the main advantage of TM-FT is its ability to directly map the boundary of the fluorophore prior to any reconstruction processes. This ThermoDots spatial information can then be used as fluorescence functional a priori information to constrain the FT image reconstruction algorithm and recover the position and concentration of the ThermoDots with high spatial resolution and quantitative accuracy.

TM-FT is not the only technique to integrate optics and ultrasound. While other techniques have also utilized focused ultrasound and a thermosensitive fluorophore, TM-FT differs in that it not only maps the size and position of the fluorophore, but also it quantifies the fluorophore distribution [12]. Two other intriguing techniques that integrate both optical and acoustic interaction are ultrasound-modulated fluorescence tomography (UMFT) and photoacoustic imaging (PAI). UMFT utilizes the direct ultrasound modulation of the optical signal in the focal zone in contrast with TM-FT, which modulates the local temperature [13]. However, the low modulation efficiency and extremely low signal-to-noise ratio (SNR) are the two main factors that make its implementation difficult. Furthermore, although micro-bubbles surface-loaded with self-quenching fluorophores have been used to enhance the contrast of UMFT, the disadvantages of using microbubbles are their instability, low circulation residence times, low binding efficiency to the area of interest, especially in the fast-flow conditions, and possible side effects of their destruction during the imaging session [14,15]. On the other hand, PAI can provide the optical absorption maps with high spatial resolution and a depth penetration of several centimeters based on ultrasonic detection of pressure waves generated by the absorption of pulsed light in elastic media [2]. However, PAI is inherently sensitive to absorption and detects a differential increase in absorption due to molecular probes compared with background absorption rather than the fluorescence signal generated by these agents. In contrast, TM-FT detects a fluorescence signal that is emitted only by the fluorescence probe, hence its sensitivity should be superior due to the high target-to-background contrast.

TM-FT is a true multimodality technique relying on both optic and acoustic interaction with the medium under investigation. We recently demonstrated the superior performance of TM-FT compared to conventional FT through simulation and experimental phantom studies [10,11,15–17]. Although agar phantoms were used to simulate the optical and mechanical properties of biological tissue, the true potential of TM-FT for preclinical and clinical applications remains unknown, as it has not been evaluated in biological tissue. In this work, we perform the first TM-FT study in chicken breast tissue to demonstrate its feasibility in biological tissue. A 1.5 mm × 5 mm inclusion filled with the ThermoDots was surgically embedded in a chicken breast slab to simulate the accumulation of the ThermoDots in the tumor due to the vascular permeability of the tumor through the enhanced permeability and retention (EPR) effect. Chicken breast, a common substitute for biological tissue in optical and ultrasound studies, was chosen due to its similarity to the optical and acoustic properties of human breast tissue [18,19]. Since the optical properties of the particular chicken breast sample used in the experiments are unknown, diffuse optical tomography (DOT) is incorporated into the existing TM-FT system to provide optical functional a priori information and constrain the TM-FT image reconstruction algorithm. These *ex vivo*

chicken breast tissue results demonstrate the ability of TM-FT to resolve small fluorescent inclusions embedded several centimeters deep in biological tissue.

2. METHODS

A. Optical Image Reconstruction Algorithm

The propagation of the excitation and fluorescent light is modeled by a combined diffusion equation that was altered to describe the temperature-dependent quantum efficiency of the ThermoDots [16]:

$$\begin{cases} -\nabla\left[D_x \nabla \Phi_x\right] - \left[\mu_{af} + \mu_{ax}\right]\Phi_x = -q_0 \\ -\nabla\left[D_m \nabla \Phi_m(\eta(T))\right] - \mu_{am}\Phi_m(\eta(T)) = -\Phi_x \eta(T)\mu_{af}, \end{cases} \quad (1)$$

where $\eta\ (T)$ denotes the temperature-dependent quantum yield and q_0 is the isotropic excitation light source. For the following variables, the subscripts x and m represent the excitation and emission wavelengths, respectively. Φ $(\mathrm{W}\cdot\mathrm{mm}^{-2})$ is the photon density, and D describes the diffusion coefficient, $D = 1/3\left(\mu_a + \mu'_s\right)$. The absorption and reduced scattering coefficients of the medium are represented by μ_a and μ'_s, respectively. μ_{af} is the absorption coefficient of the fluorophore and is directly related to its concentration. The combined diffusion equation is solved with the finite element method (FEM) using a mesh that consists of 6034 nodes and 11,775 triangular elements. Details of this method have been published previously [4].

B. Instrumentation

The experiment was performed with a custom-built FT system [9]. A 790 nm (300 mW, Thorlabs, NJ) laser modulated by a 100 MHz RF signal was used to illuminate the chicken breast. Due to multiple losses within the system, approximately 50 mW reaches the surface of the imaged medium. A photomultiplier tube (PMT) (R7400U-20, Hamamatsu) was chosen to detect the fluorescence emission signal due to its high gain together with a bandpass optical filter (830 nm, 10 nm bandwidth). Its output signal was amplified and monitored with a network analyzer (Agilent Technologies, California). Additionally, the system was modified in order to divert the detected excitation light into a second identical PMT to collect DOT measurements. A focused ultrasound transducer (H-102, Sonic Concepts Inc., Washington) centered at 1.0 MHz was mounted on an automated computer programmed xy translational stage system to scan the chicken breast sample. A third manual stage allowed height adjustments. As necessitated by the utilization of the acoustic waves, the transducer and optical interface were immersed in water (Fig. 1).

To generate the exogenous a priori information, the transducer was turned on to induce a 4°C temperature increase at the focal zone and scanned over a 50 mm × 25 mm area in 29 min [16]. The transducer was scanned at a speed of 4.16 mm/s to avoid the effect of heat diffusion. The sampling rate of the network analyzer corresponds to one measurement per 0.25 mm. The full width at half-maximum (FWHM) was used as a threshold to create a binary map of the position of the ThermoDots with high spatial resolution.

C. ThermoDots

The ThermoDots are provided by our collaborators at InnoSense LLC (Torrance, California) and consist of encapsulating the near NIR fluorophore ICG inside thermo-responsive Pluronic-F127 polymeric micelles. The ThermoDots are characterized to determine their fluorescence signal intensity response to temperature. The ThermoDots used in this study exhibited a 15× increase in fluorescence signal from a 4°C change in temperature. In this *ex vivo* study, the experiment was performed at room temperature, and the focused ultrasound was set to induce a 4°C change in temperature at its focal spot to maximize the fluorescence signal change. Further details on the ThermoDots preparation and characterization can be found in Kwong *et al.* [20].

D. Phantom Studies

For this study, a chicken breast was cut into a 30 mm × 40 mm × 90 mm slab and centered in the middle of the sample holder (100 mm × 40 mm × 100 mm). The middle of the chicken breast slab was aligned with the optical fiber plane using a tissue mimicking agar slab, as seen in Fig. 1. The chicken breast was surrounded with an optical matching fluid and sealed with a clear acoustically transparent plastic to reduce reflection of the focused ultrasound waves. The agar slab and matching fluid were prepared using intralipid (0.5%) and India Ink (Winsor and Newton, UK) to, respectively, mimic the tissue reduced scattering and absorption properties: $\mu'_s = 0.6\,\mathrm{mm}^{-1}$ and μ_a 0.008 mm^{-1}. A small clear acoustically transparent plastic tube (1.5 mm × 5 mm) was filled with the ThermoDots solution, 836 nM ($\mu_{af} = 0.02\ \mathrm{mm}^{-1}$), and surgically em-bedded inside the chicken breast slab. The tube was aligned along the fiber plane and centered between the source and detector located third from the left, as seen in Fig. 1.

3. RESULTS AND DISCUSSION

To test the feasibility of TM-FT in imaging biological tissue, we investigated the performance of TM-FT to accurately recover the size, shape, position, and concentration of the inclusion filled with ThermoDots embedded inside the chicken breast slab. The fluorophore absorption maps recovered with conventional FT and TM-FT were compared to the true value. First, DOT was used to recover the absorption and reduced scattering coefficients of the chicken breast sample, as described previously [21]. As the absorption and reduced scattering coefficients of the *ex vivo* chicken breast at the excitation and emission wavelengths are nearly equal (~1% difference), μ_a and μ'_s maps were acquired at the excitation wavelength, 790 nm for this study [22]. In addition, due to the low optical absorption contrast (<2×) and small size (<5%) of the inclusion compared to the background chicken breast, the obtained optical absorption and scattering maps were mostly homogeneous. The averaged optical properties of the chicken breast obtained were $\mu_a = 0.014\ \mathrm{mm}^{-1}$ and $\mu'_s = 0.517\ \mathrm{mm}^{-1}$. Next, conventional FT measurements were acquired, and the reconstructed DOT optical properties were used as optical functional a priori information in the conventional FT reconstruction program to identify the location of the ThermoDots. Then, the focused ultrasound scan was used to create a binary map of the position of the fluorescence tube with high spatial resolution. Finally, this binary map was

implemented as a soft a priori with the previous fluorescence data to reconstruct the concentration of the ThermoDots [23].

Figure 2 shows the recovered fluorescence absorption maps (obtained with DOT optical functional a priori) comparing conventional FT and TM-FT with the true fluorescence absorption value in the tube. As seen in Fig. 2(b), conventional FT recovers a fluorescent distribution 3× larger in the *x*-axis and 5.5× larger in the *y*-axis directions than the true size of the tube. Consequently, since the recovered fluorescence is attributed to a larger area, the fluorescence absorbance is underestimated at 0.006 mm^{-1} (3.4× smaller than the true fluorescence absorbance set to 0.02 mm^{-1}). However, the binary mask generated from the focused ultrasound scan in Fig. 2(c) local-izes the ThermoDots' position prior to any reconstruction process. To recover the concentration of the inclusion, this binary mask is used as fluorescence functional soft a priori and combined with the DOT optical functional a priori information to solve the FT inverse problem. The resultant TM-FT fluorescence absorption map [Fig. 2(d)] illustrates the superior spatial resolution and quantitative accuracy compared to conventional FT. TM-FT not only recovers the true size, shape, and position of the true fluorescent inclusion, but also recovers the exact fluorescence absorption at 0.02 mm^{-1} and concentration of 836 nM.

The limited resolution of conventional FT can be seen in Fig. 2(b) as it recovers an ellipsoid shaped fluorescence distribution compared to the true rectangular distribution of the ThermoDots tube. However, TM-FT relies on the acoustics waves from the focused ultrasound transducer and is therefore not constrained by the same scattering and absorption limitations as optical waves. This can be seen in the superior spatial resolution of the TM-FT results. Consequently, TM-FT is more accurate at recovering the correct shape and position of the ThermoDots. As seen in Fig. 3, although irregularly shaped, the TM-FT fluorescence distribution is confined mainly within the known boundary (green line) and corresponds well with the true ThermoDots distribution. The irregularities in the outline are a result of the shape of the mesh elements.

TM-FT nearly recovers the exact size of the 1.50 mm diameter by 5.00 mm long tube. TM-FT reconstructs the exact length of the tube in the *x* axis and slightly overestimated the diameter by a mere 0.25 mm. Although irregularly shaped, Fig. 4 shows the profiles of the ThermoDots distribution in the x and y axes, which were carried out where the fluorescent distribution was the largest [blue dashed lines in Fig. 2(a)]. The recovered TM-FT fluorescence distribution is shifted 0.25 mm to the left on the *x* axis and slightly upwards by 0.125 mm on the *y* axis. This might be the result of the interpolation from the mesh to the Cartesian grid image. Nevertheless, with only 0.25 mm or less difference in position, TM-FT can accurately recover the correct position of the ThermoDots in biological tissue.

In comparison, for conventional FT, the center of the recovered fluorophore distribution is shifted 1.25 mm to the right in the *x*-axis direction and exactly aligned in the *y*-axis direction. The recovered size of the ThermoDots distribution is greatly overestimated at 15.75 mm in the *x* axis and 8.25 mm in the *y* axis. In general, the spatial resolution of conventional FT in the *y* direction is expected to be lower than the x direction due to the trans-illumination configuration of the source and detector fibers. Conversely, TM-FT is

unaffected, as the spatial resolution of TM-FT is primarily determined by the spa-tial resolution of focused ultrasound. In addition, the accuracy of FT and TM-FT strongly depends on the accuracy of their forward problem to model the light propagation within the medium. When the optical properties of chicken breast were taken from literature and assumed $\left(\mu_a = 0.01\text{mm}^{-1}\right.$ and $\left.\mu'_s = 0.3\text{mm}^{-1}\right)$, there was a 30% error in the recovered fluorescence absorption [22]. However, when the correct absorption and reduced scattering values were obtained from the DOT measurements, the error decreased to 0.45%.

4. CONCLUSION

In conclusion, this chicken breast study demonstrates the ability of TM-FT to accurately recover the correct size, shape, position, and concentration of the ThermoDots inclusion in biological tissue. Our previous studies were performed in agar phantoms that mimicked but did not accurately represent the true optical and mechanical properties or heterogeneity of biological tissue. As this technique heavily relies on both optical and acoustic waves, a more accurate model is needed to verify the feasibility of TM-FT in biological tissue. Chicken breast was chosen, as it is a common substitute for human breast tissue in optical and ultrasound studies [18,19]. Consequently, this study was the first to demonstrate that TM-FT can be used in biological tissue. The results show that TM-FT was able to recover the correct size and position of the ThermoDots with submillimeter error and recover the true ThermoDots absorption with less than 0.5% error. These promising results demonstrate the feasibility of TM-FT in biological tissue, and with further optimization of the ThermoDots to target specific receptors, opens up the possibility for high spatial resolution whole-body *in vivo* small animal imaging in the future.

Acknowledgments

Funding. National Institutes of Health (NIH) (F31CA171915, P30CA062203, R01EB008716, R33CA120175, SBIR HHSN261201300068C); University of California, Irvine (UCI); Fulbright Commission (Visiting Scholar).

REFERENCES

1. Leblond F, Davis SC, Valdés PA, and Pogue BW, “Preclinical whole-body fluorescence imaging: review of instruments, methods and applications,” J. Photochem. Photobiol. B 98, 77–94 (2010). [PubMed: 20031443]
2. Wu H-I and Wang LV, Biomedical Optics: Principles and Imaging, 1st ed. (Wiley-Interscience, 2007).
3. Davis SC, Dehghani H, Wang J, Jiang S, Pogue BW, and Paulsen KD, “Image-guided diffuse optical fluorescence tomography implemented with Laplacian-type regularization,” Opt. Express 15, 4066–4082 (2007). [PubMed: 19532650]
4. Lin Y, Yan H, Nalcioglu O, and Gulsen G, “Quantitative fluorescence tomography with functional and structural a priori information,” Appl. Opt 48, 1328–1336 (2009). [PubMed: 19252634]
5. Guvan M, Yazici B, and Ntziachristos V, “Fluorescence optical tomography with a priori information,” Proc. SPIE 6431, 643107 (2007).
6. Saxena V, Sadoqi M, and Shao J, “Enhanced photo-stability, ther-mal-stability and aqueous-stability of indocyanine green in polymeric nanoparticulate systems,” J. Photochem. Photobiol. B 74, 29–38 (2004). [PubMed: 15043844]

7. Kim T, Chen Y, Mount CW, Gombotz WR, Li X, and Pun SH, "Evaluation of temperature-sensitive, indocyanine green-encapsulating micelles for noninvasive near-infrared tumor imaging," Pharm. Res 27, 1900–1913 (2010). [PubMed: 20568000]
8. Escobar-Chávez JJ, López-Cervantes M, Naïk A, Kalia YN, Quintanar-Guerrero D, and Ganem-Quintanar A, "Applications of thermo-reversible pluronic F-127 gels in pharmaceutical formulations," J. Pharm. Pharm. Sci 9, 339–358 (2006). [PubMed: 17207417]
9. Choi SH, Lee J-H, Choi S-M, and Park TG, "Thermally reversible pluronic/heparin nanocapsules exhibiting 1000-fold volume transi-tion," Langmuir 22, 1758–1762 (2006). [PubMed: 16460102]
10. Lin Y, Bolisay L, Ghijsen M, Kwong TC, and Gulsen G, "Temperature-modulated fluorescence tomography in a turbid media," Appl. Phys. Lett 100, 073702 (2012).
11. Lin Y, Kwong TC, Bolisay L, and Gulsen G, "Temperature-modulated fluorescence tomography based on both concentration and lifetime contrast," J. Biomed. Opt 17, 056007 (2012). [PubMed: 22612130]
12. Cheng B, Bandi V, Wei MY, Pei Y, D'souza F, Nguyen KT, Hong Y, and Yuan B, "High-resolution ultrasound-switchable fluores-cence imaging in centimeter-deep tissue phantoms with high signal-to-noise ratio and high sensitivity via novel contrast agents," PLoS One 11, e0165963 (2016). [PubMed: 27829050]
13. Yuan B and Liu Y, "Ultrasound-modulated fluorescence from rhod-amine B aqueous solution," J. Biomed. Opt 15, 021321 (2010). [PubMed: 20459241]
14. Yuan B, "Ultrasound-modulated fluorescence based on a fluoro-phore-quencher-labeled microbubble system," J. Biomed. Opt 14, 024043 (2009). [PubMed: 19405771]
15. Klibanov AL, "Ligand-carrying gas-filled microbubbles: ultrasound contrast agents for targeted molecular imaging," Bioconjugate Chem 16, 9–17 (2005).
16. Nouizi F, Kwong TC, Cho J, Lin Y, Sampathkumaran U, and Gulsen G, "Implementation of a new scanning method for high-resolution fluorescence tomography using thermo-sensitive fluores-cent agents," Opt. Lett 40, 4991–4994 (2015). [PubMed: 26512501]
17. Kwong TC, Nouizi F, Lin Y, Cho J, Zhu Y, Sampathkumaran U, and Gulsen G, "Experimental evaluation of the resolution and quan-titative accuracy of temperature-modulated fluorescence tomogra-phy," Appl. Opt 56, 521–529 (2017). [PubMed: 28157909]
18. Sultan SF, Shorten G, and Iohom G, "Simulators for training in ultrasound guided procedures," Med. Ultrason 15, 125–131 (2013). [PubMed: 23702502]
19. Yao G and Wang LV, "Theoretical and experimental studies of ultra-sound-modulated optical tomography in biological tissue," Appl. Opt 39, 659–664 (2000). [PubMed: 18337939]
20. Kwong TC, Nouizi F, Sampathkumaran U, Zhu Y, Alam MM, and Gulsen G, "Activatable thermo-sensitive ICG encapsulated Pluronic nanocapsules for temperature sensitive fluorescence tomography," Proc. SPIE 9339, 93390C (2015).
21. Lin Y, Gao H, Nalcioglu O, and Gulsen G, "Fluorescence diffuse optical tomography with functional and anatomical a priori information: feasibility study," Phys. Med. Biol 52, 5569–5585 (2007). [PubMed: 17804882]
22. Alhamami M, Kolios MC, and Tavakkoli J, "Photoacoustic detection and optical spectroscopy of high-intensity focused ultrasound-induced thermal lesions in biologic tissue," Med. Phys 41, 053502 (2014). [PubMed: 24784408]
23. Yalavarthy PK, Pogue BW, Dehghani H, Carpenter CM, Jiang S, and Paulsen KD, "Structural information within regularization matrices improves near infrared diffuse optical tomography," Opt. Express 15, 8043–8058 (2007). [PubMed: 19547132]

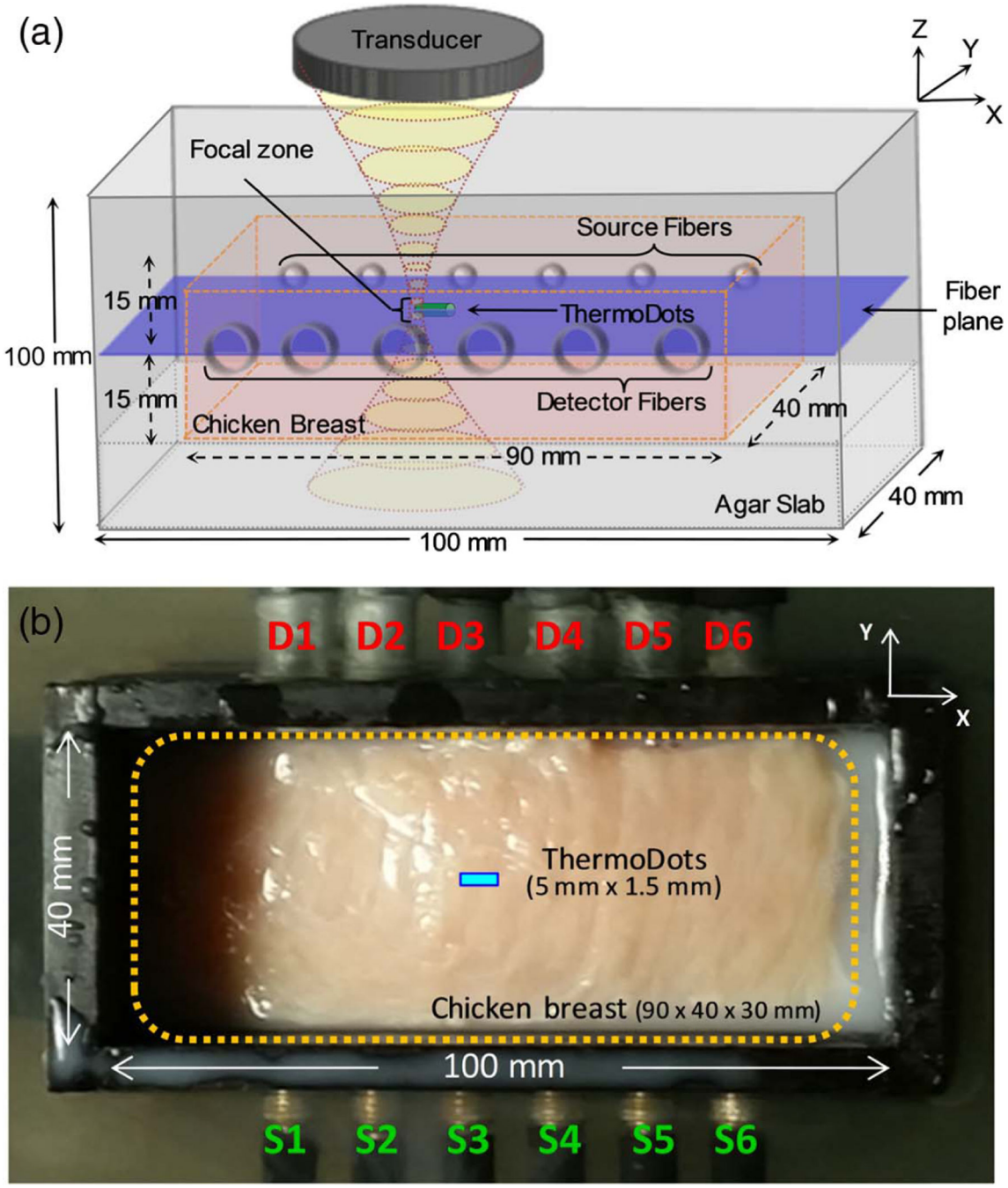

Fig. 1.

(a) 3D schematic showing the sample holder and the focused ultrasound transducer. The transducer produces a focal zone of ~1.33 mm diameter (*xy*) and 10 mm in length (*z*). The center of the focal zone, ThermoDots inclusion (green tube), and chicken breast slab (pink box) are aligned in the fiber plane (blue plane) defined by the source and detector optical fibers. The chicken breast rested on an agar slab and is surrounded by an optical matching fluid. (b) Experimental setup of chicken breast sample in phantom holder with source and detector fibers.

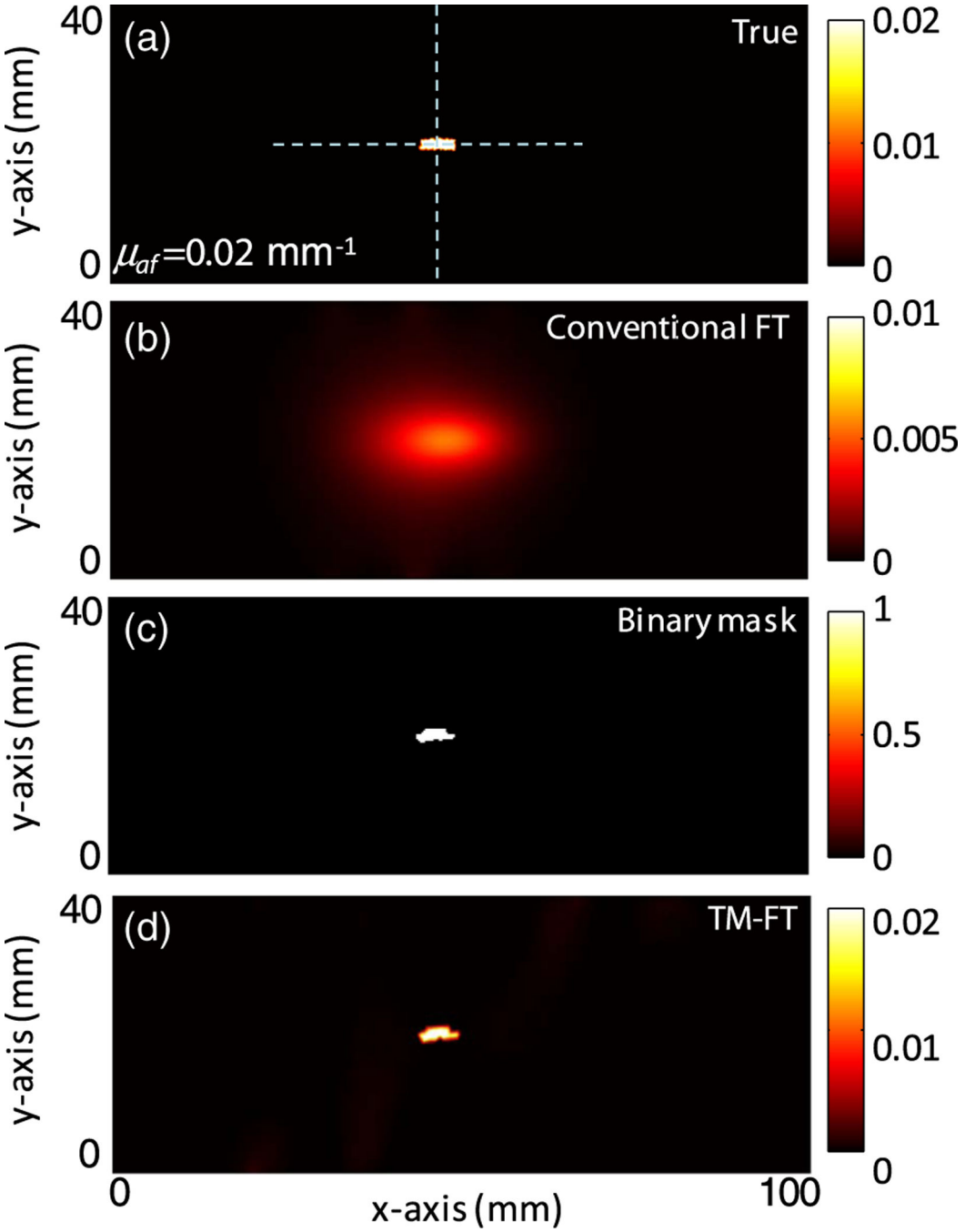

Fig. 2.

ThermoDots μ_{af} maps in fiber plane. (a) True ThermoDots distribution. (b) Conventional FT fluorescence map with DOT a priori. (c) Fluorescence binary mask used to guide and generate the (d) TM-FT fluorescence absorption map with DOT a priori. The blue dashed lines show the profiles displayed in Fig. 4. Color bar units are mm^{-1}.

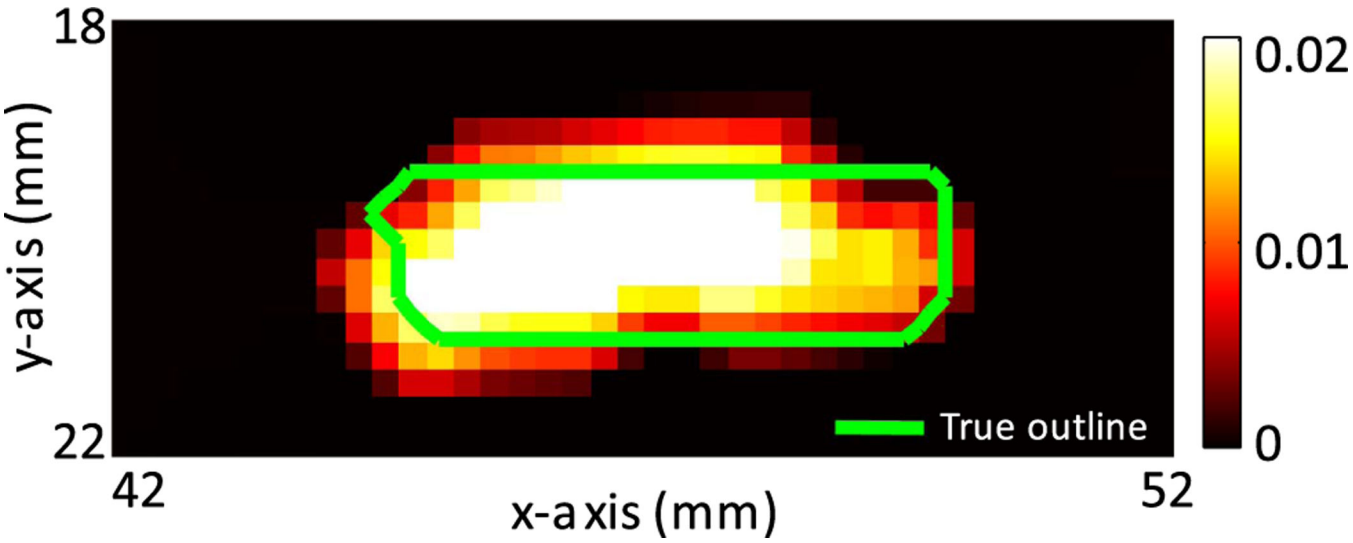

Fig. 3.

Close-up of the recovered μ_{af} map with the true ThermoDots boundary outlined (green). A very good agreement is obtained between the shape, size, and position of the ThermoDots recovered with TM-FT and the true value. The pixel size is 0.25 mm × 0.25 mm. The color bar has units of mm^{-1}.

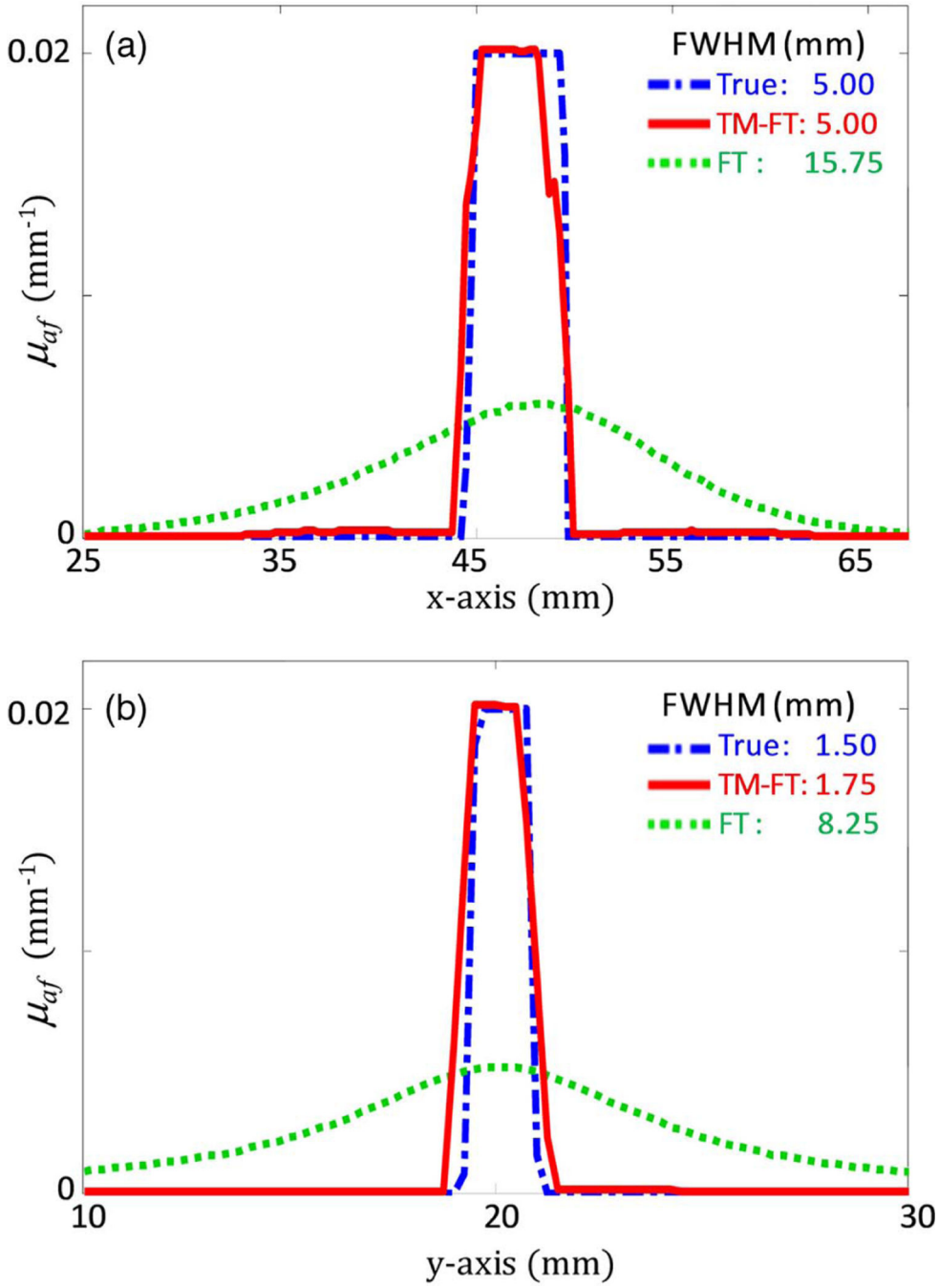

Fig. 4.

Profiles of the ThermoDots recovered μ_{af} maps along the blue dashed lines in Fig. 3(a). The profiles along the (a) x axis and (b) y axis show that the size of the fluorescent target is accurately recovered using TM-FT (red line). Conventional FT (green dotted line) is severely overestimated in size and underestimated in absorption value compared to the true value (blue dot-dashed line).